2.3 TEMPORAL SPECTRA OF EARTH RADIATION BUDGET COMPONENTS

Takmeng Wong*
Atmospheric Sciences Division, NASA Langley Research Center
Hampton, Virginia

G. Louis Smith
Virginia Polytechnic Institute and State University
NASA Langley Research Center
Hampton, Virginia

1. INTRODUCTION

Continuous monitoring of the Earth's radiation field at the top of the atmosphere (TOA) is essential for understanding climate and climate variability on Earth. To achieve this important science goal, the National Aeronautic and Space Administration (NASA) has begun the Clouds and the Earth's Radiant Energy System (CERES) project (Wielicki et al. 1996), which consists of earth radiation budget instrument packages flying on three different satellites, beginning with the Tropical Rainfall Measuring Mission satellite in November 1997, the Earth Observing System (EOS) Terra spacecraft in December 1999, and the EOS Aqua satellite in summer of 2002. Building on the successful Earth Radiation Budget Experiment (ERBE) project (Barkstrom 1984), this multi-satellite Earth radiation budget mission will provide the scientific community with necessary information for monitoring and understanding the earth's radiation environment well into the 21th century.

After two months of initial routine checkup, the two CERES instruments installed aboard the NASA EOS Terra spacecraft begin taking scientific observations on February 26, 2000. They have since provided global broadband measurements of outgoing longwave radiation (OLR) and of reflected solar radiation (RSR) from the Earth for over one and half years. When daily global maps of these parameters are viewed in sequence as a movie for the first year, one sees variations of OLR and RSR due to synoptic scale dynamics. When weekly means are computed so as to filter out synoptic variations, one sees variations at a wide range of temporal and spatial scales. These longer-term variations are of special interest because their time scales are well beyond the usual 7 to 10 day life of synoptic variations and cover a latitude range up to 30 degrees north and south. This paper demonstrates some techniques for studying variations in time and space of meteorological variables such as TOA radiation fields. Specifically, we like to examine the structures of both OLR and RSR with periods of more than 20 days. Section 2 describes the source of radiation budget data and the analysis technique used in this study. Section 3 shows the analysis results for both TOA OLR and RSR field. Discussion and concluding remarks are given in section 4.

Corresponding author address: Dr. Takmeng Wong, Mail Stop 420, NASA Langley Research Center, Hampton, VA 23681-2199; e-mail: takmeng.wong@larc.nasa.gov.

2. DATA AND ANALYSIS TECHNIQUES

Global regional daily mean broadband all-sky OLR and RSR data are used in this paper to study the temporal features of TOA radiation fields. These data are extracted from the first full year of CERES/Terra ERBE-like Edition 1 ES-4G dataset and cover the period between March 1, 2000 and February 28, 2001. The CERES ERBE-like global regional daily mean data consist of values of TOA radiation for each of the 10,368 individual 2.5-degree regions on Earth covering all area from North Pole to South Pole. In addition, values of TOA radiation from the two CERES instruments on Terra spacecraft are combined together to form a single arithmetic average for this study.

In order to examine the temporal structures of the TOA radiation data, time histories of OLR and RSR are Fourier-analyzed for each 2.5-degree region of the globe. From these results the temporal spectra are computed for each region. The longitudinal structure of the temporal spectrum can be examined by use of the Hovmueller diagram modified to the Fourier domain. The question then arises: how does one examine the temporal spectrum for a map? One approach is to integrate the spectrum over a selected frequency domain, e.g. corresponding to 20 to 60 days, and form maps of these partial variances. Another approach is to form a movie in which the temporal frequencies are

viewed in sequence, i.e one exchanges the time domain for the Fourier domain. The results of these analyses are highlighted in section 3 below.

3. EXAMINATION OF DATA

3.1 *OLR Data*

Figure 1a and 1b show the time histories of OLR for a point in the Indian Ocean (0^{o}N, 86^{o}E) and a point in Eastern Pacific Ocean (8^{o}S, 248^{o}E) for the one year period between March 1, 2000 and February 28, 2001. While the OLR time series at the point over Indian Ocean show significant variability over the span of the data period, the variability of OLR at the point over the Eastern Pacific Ocean, with the exception during the transitional months between mid-February and end of April, is very small.

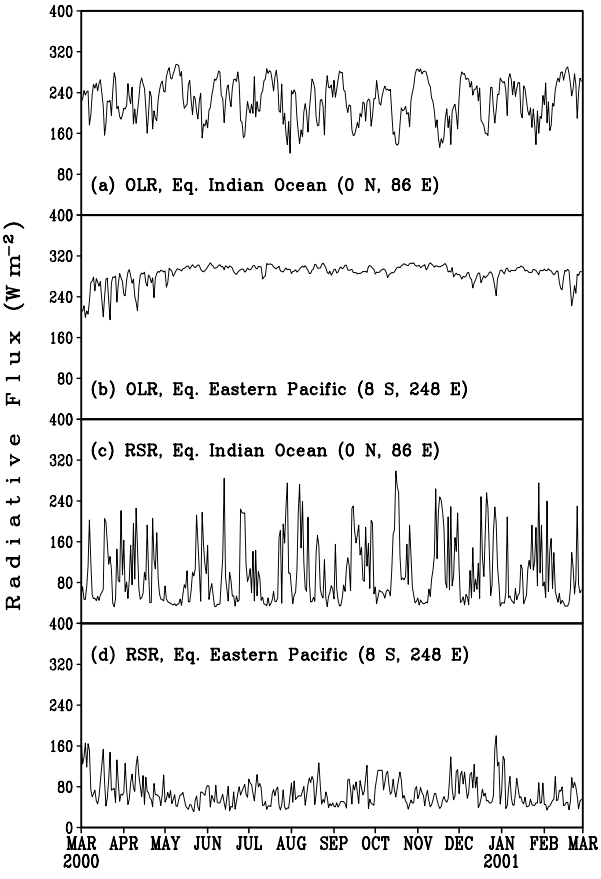

FIG. 1. Variation of OLR (a and b) and RSR (c and d) with time for a point in the Indian Ocean (0^{o}N, 86^{o}E) and a point in Eastern Pacific Ocean (8^{o}S, 248^{o}E) for the one year period between March 1, 2000 and February 28, 2001.

Figure 2a shows the temporal spectrum of OLR for the same two locations. The Indian Ocean site has a definite spectral peak at 0.03 day^{-1}, corresponding to a period of 30 days. The traditional monthly mean radiation data product makes this variation invisible. For frequencies greater than 0.05 days^{-1} (20 day period) the spectrum seems to decrease linearly in this log-log plane, suggesting a power law relation. The OLR temporal spectrum for the Eastern Pacific Ocean site has no pronounced peak in the 0.03 day^{-1} range but does decrease for frequencies greater than 0.05 days^{-1}.

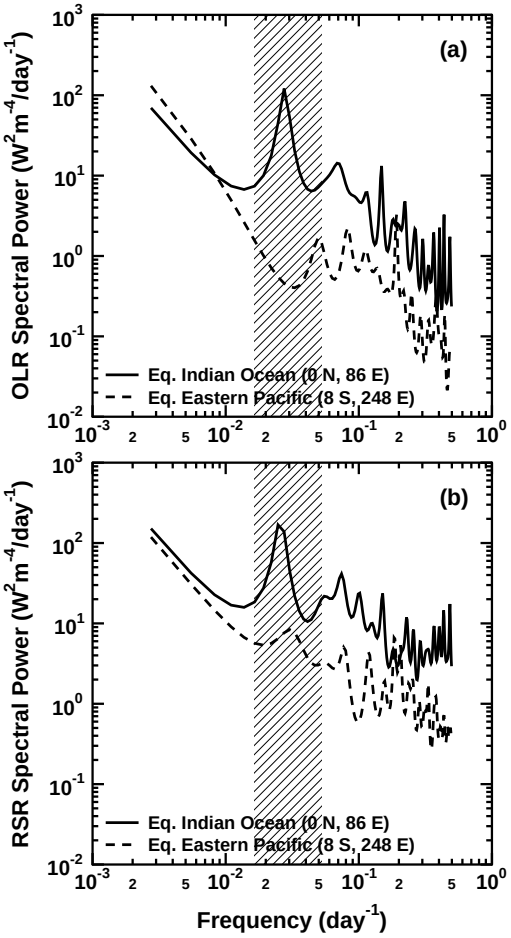

FIG. 2. Variation of spectral power of (a) OLR and (b) RSR with frequency based on time histories given in Fig. 1 for a point in the Indian Ocean (0^{o}N, 86^{o}E; solid lines) and a point over Eastern Pacific Ocean (8^{o}S, 248^{o}E; dashed lines). The shaded areas highlight the intraseasonal frequency domain with period between 20 to 60 days.

Figure 3a is a Fourier-Hovmueller diagram showing the variation of spectral power with longi-

tude at the Equator. Between 60°E and 180°, there is considerable power, which peaks in the range of 30 to 40 days over the Indian Ocean. Further east is another active region around 140°E. Beyond these 2 active regions there is very little spectral power except for the seasonal cycles. This peak may be the Madden-Julian oscillation (MJO; Madden and Julian, 1972). The lack of power in other longitudes indicates that the MJO propagates through these regions as a dry pressure wave, but moves through the active regions as a moist process which provides its energy.

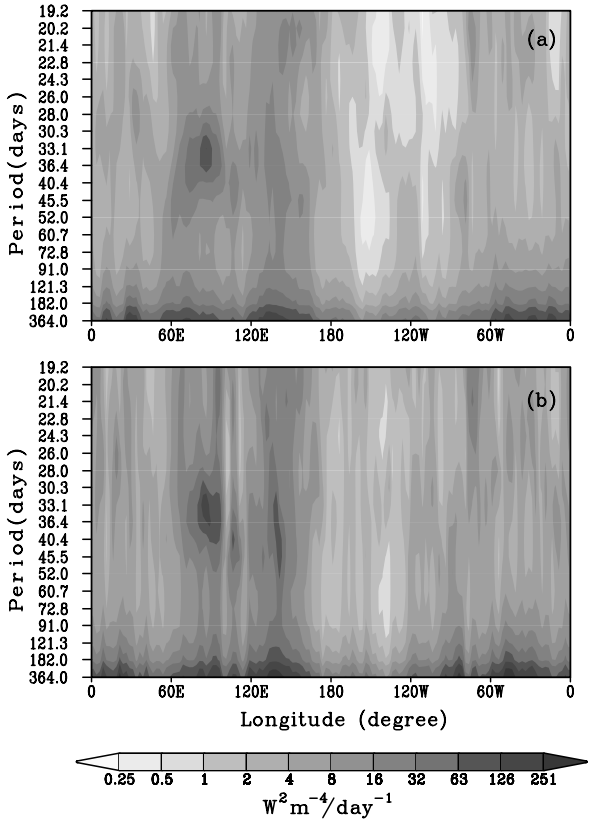

FIG. 3. Dependence of spectral power with longitude around Equator for (a) OLR and (b) RSR.

In order to map the spectral power, the spectrum is integrated from 0.0167 (60 day period) to 0.05 day^{-1} (20 day period) for each 2.5 degree region. The spectral power integrated over the full range is the variance, so the integral over a restricted range is a partial variance. For the selected frequency range, the partial variance is the intraseasonal contribution. Figure 4a is a map of the partial variance of OLR. There is a large partial variance in the Tropics over the west Indian Ocean, the area around the Maritime Continent, the Inter-Tropical Convergence Zone (ITCZ) and the Southwest Pacific Convergence Zone. In the Atlantic Ocean the variation of the ITCZ appears as changes of the easterly outflow from North Africa towards the Caribbean region. There are also large changes in the OLR for the Amazon region. There is very little intraseasonal variation over the subsidence zone along the Equator between the dateline and the west coast of South America. The intraseasonal partial variance extends beyond the Tropics but is small at latitudes greater than 50° in both hemispheres.

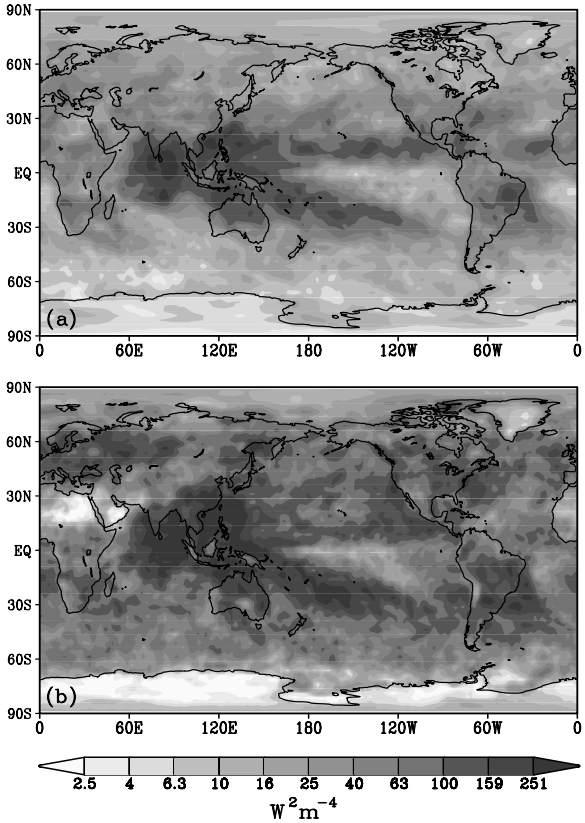

FIG. 4. Map of spectrum integrated from 6 to 18 cycles per year (20 to 60 day periods) for (a) OLR and (b) RSR.

3.2 *RSR Data*

Reflected solar radiation (RSR) tells a different story. Whereas OLR variations at low latitudes are indicative of high (and cool) clouds, clouds at any vertical level in the atmosphere will change RSR. Figure 1c and 1d show the time histories of RSR for the same two sites over the Indian and Eastern Pacific Ocean and during the same period considered in Fig. 1a and 1b. The variabilities of the RSR fields look similar to those of the OLR fields with

high variability for the point over the Indian Ocean and low variability for the point over Eastern Pacific Ocean. In addition, the magnitudes of the RSR variability are higher than those of the OLR fields.

Figure 2b shows the temporal spectrum of RSR for these two locations. For the Indian Ocean site the pronounced peak again appears for 0.030 day^{-1} (30 day period). Whereas the Eastern Pacific Ocean point did not show a peak in the OLR spectrum at intraseasonal frequencies, there is a peak in the RSR spectrum near 0.040 day^{-1} (25 day period). Because this peak does not appear in the OLR spectrum, it is attributed to low clouds. The spectrum for RSR at high frequencies does not decrease as rapidly as did the OLR.

Figure 3b shows the variation of spectral power for RSR with longitude around the Equator. It is quite similar to that for OLR, except with a broader distribution. The RSR spectra at 100°E and 140°E are nearly flat at a high level.

Figure 4b is a map of the partial variance of RSR, defined as before as the integral of the spectral power from 0.0167 to 0.05 day^{-1}. The areas of high OLR variability are also areas of high RSR variability. The subsidence region along the Equator between the dateline and the west coast of South America shows variations of the RSR, indicating that these variations are due to changes of low clouds. There are similar differences over the Pacific Ocean west of the coast of North America. There are also large changes over Europe, where little change appeared for OLR, indicating here that the variations are due to low clouds. Because they reflect solar radiation without changing the OLR, low clouds affect the net radiative balance of a region. The OLR partial variance is small poleward of 40° of the Equator, but the RSR intraseasonal variations extend well beyond 60° latitude in both hemispheres.

4. DISCUSSION AND CONCLUSIONS

An examination of OLR and RSR data shows Intraseasonal variations, especially in the Tropics, with effects propagating to higher latitudes. These intraseasonal variations are due to weather patterns which persist well beyond the traditional limit of predictability and require research to understand. Due to the duration of the patterns, there is ample time for radiation to interact with dynamics in their development.

Examination of daily OLR maps in sequence over a 1-year period shows a variety of motions with spectral power between 20 and 60 days. These motions are filtered out in monthly mean data products, which are useful for studying interannual variations. These processes are strong as far as 30° from the Equator and cover half the Earth. They are more than simply Madden-Julian oscillations, which, being Kelvin waves, are concentrated near the Equator. They are strong over the Indian Ocean and subcontinent, Southeast Asia and Indonesia and affect over 2 billion people.

Studies of the interaction of radiation with climate processes must move beyond the monthly mean (a goal from the 1970's) and consider intraseasonal processes. Study is needed to define the reasons for these variations of OLR and RSR and the effects of these variations on the dynamics of the ocean/atmosphere/land system. In the Tropics, OLR varies primarily due to cloud changes. The strong regional dependence of the activity, or conversely inactivity, indicates that the processes are driven by interaction with the surface, e.g. through orography, hydrology or sea surface temperature. Because these processes have times of 20 to 60 days associated with them, there must be predictive capability possible for this period. Due to their duration, these processes must heavily involve radiation. In order to make predictions possible over the extended time period, continued observations of radiation budget will be required.

Acknowledgments. This work was supported by NASA Earth Science Enterprise through the CERES project at NASA Langley Research Center and by cooperative agreement NCC-1-405 with Virginia Polytechnic Institute and State University. CERES data were provided by NASA Langley Atmospheric Sciences Data Center.

REFERENCES

Barkstrom, B. R., 1984: The Earth Radiation budget Experiment (ERBE). *Bull. Amer. Meteor. Soc.,* **65**, 1170-1185.

Madden, R. A., and P. R. Julian, 1972: Description of Global-Scale Circulation Cells in the Tropics with a 40-50 Day Period. *J. Atmos. Sci.*, **29**, 1109-1123.

Wielicki, B. A., B. R. Barkstrom, E. F. Harrison, R. B. Lee III, G. L. Smith, and J. E. Cooper, 1996: Clouds and the Earth's Radiant Energy System (CERES): An Earth Observing System experiment. *Bull. Amer. Meteor. Soc.*, **77**, 853-868.